Available online at www.sciencedirect.com
ScienceDirect
Energy Procedia 2 (2010) 3–7
Energy Procedia
www.elsevier.com/locate/procedia

E-MRS Spring meeting 2009, Symposium B

Structural And Electrical Properties Of Nanostructured Silicon Carbon Films

G. Ambrosone[1,2*]*, D.K. Basa[3], U. Coscia[4,2], L. Santamaria[2], N. Pinto[5], M. Ficcadenti[5], L. Morresi[5], L. Craglia[5], R. Murri[5]

[1]INFM-CNR, CRS-Coherentia, Complesso MSA, via Cintia, I-80126, Napoli, Italy
[2]Dipartimento di Scienze Fisiche, Università di Napoli "Federico II", Complesso Universitario MSA, via Cintia, I-80126 Napoli, Italy
[3]Department of Physics, Utkal University, Bhubaneswar-751004, India
[4]CNISM Unita' di Napoli, Complesso MSA, via Cintia, I-80126, Napoli, Italy
[5]Dipartimento di Fisica, Universita' di Camerino, via Madonna delle Carceri 9, 62032 Camerino, Italy

Received 1 June 2009; received in revised form 1 December 2009; accepted 20 December 2009

Abstract:

The effect of the rf power on the structural and electrical properties of nanostructured silicon carbon films deposited by Plasma Enhanced Chemical Vapour Deposition system, using silane and methane gas mixture highly diluted in hydrogen, has been investigated. The structural and electrical properties are found to depend strongly on rf power. The increase of the rf power decreases the size of the silicon crystallites as well as the crystalline fraction and increases the carbon content in the films. The study not only indicates the correlation between crystalline fraction and the electrical conductivity but also reveals the presence of nanocrystallites in the films deposited at high rf power.

Keywords: Silicon carbon; nanocrystals; Raman spectroscopy; X ray diffraction; Infrared spectroscopy; electrical properties

1. Introduction

The nanostructured silicon carbon films composed of submicron Si crystallites embedded in amorphous matrix are very promising for device applications such as thin film transistors, thin film solar cells and light emitting diodes [1-3]. Indeed these materials show higher electrical conductivity, optical transparency, dopant activation and long term stability as compared to the amorphous counterpart [4-6]. Device fabrication requires low deposition

* Corresponding author. Tel.:+39 081 676101; fax:+039 081 676346.
E-mail address: ambrosone@na.infn.it.

doi:10.1016/j.egypro.2010.07.003

temperature to avoid damaging of the substrate as well as the interfaces. It has been reported that microcrystalline and nanocrystalline silicon carbon films have been grown by Plasma Enhanced Chemical Vapour Deposition (PECVD) at substrate temperature less than 400°C [6-16]. The doped microcrystalline silicon carbon films have been widely investigated, while the undoped materials, potentially suitable as active layer for multiple junction solar cells, UV photodectors and light emitting diodes, have not been well studied. Since rf power plays an important role to tailormade the properties of the amorphous and microcrystalline silicon carbon, in this work we have investigated the effects of rf power on the structural and electrical properties of silicon carbon films deposited at relatively low substrate temperature of 250°C by PECVD technique, using silane and methane gas mixture highly diluted in hydrogen.

2. Experimental details.

Hydrogenated silicon-carbon films were prepared in a high vacuum 13.56 MHz capacitively coupled PECVD system. Films were simultaneously deposited onto different substrates: 7059 Corning glass for Raman, X-ray diffraction (XRD) and electrical measurements, while crystalline Si(100) for infrared (IR) and nuclear measurements. Films were grown by silane (SiH_4) and methane (CH_4) gas mixture highly diluted in hydrogen (H_2). For the depositions of the films the pressure, the total gas flow rate, the substrate temperature, the methane fraction, $[CH_4]/([SiH_4]+[CH_4])$, and the hydrogen dilution, $[H_2]/([SiH_4]+[CH_4])$, were fixed at 227 Pa, 300 sccm, 250 °C, 0.50 and 250 respectively, while the rf power, *w,* was varied from 10 to 65 W (rf power density range 67-433 mW/cm^2).

Raman spectra of the studied films were obtained in 200 – 2000 cm^{-1} range using a Micro-Raman Renishaw spectrophotometer equipped with a cooled CCD detector and an Argon laser excitation at 514.5 nm. The samples were characterized by XRD measurements carried out with a Brucker D-5000 diffractometer, using a CuK_a radiation source. Crystallite sizes were determined using the well known Scherrer formula. Elemental compositions of samples were obtained from nuclear techniques, such as Rutherford backscattering (RBS), elastic recoil detection analysis (ERDA) and nuclear reaction analysis (NRA). IR measurements were carried out using Fourier Transform Infrared (FTIR) Perkin Elmer spectrophotometer in the range 400-4000 cm^{-1}.

Dark conductivity, σ_d, and photoconductivity, σ_{ph}, under white light of 100 mW/cm^2 (AM1 conditions) were measured at room temperature in a coplanar configuration using Keithley 617 electrometer. Film conductivity as a function of the temperature was measured from room temperature to about 500 K. The measurements were carried out in a furnace, with a thermal stability better than 0.1 K, and in high vacuum, at a pressure < 10^{-4} Pa. Conductivity was measured during consecutive heating and cooling runs by a PC controlled system after the stabilization of the measurement temperature. The heating and cooling rates were about 5×10^{-3} K/s.

3. Results and discussion

Raman, XRD and IR measurements were undertaken to characterize the structure of the studied hydrogenated silicon carbon films, deposited by varying the rf power. Raman spectra of the samples are shown in Fig. 1. It is known that the bulk crystalline silicon gives a narrow peak at 520 cm^{-1} which is the characteristic of Si-Si TO (transverse optical) mode, while amorphous silicon exhibits a broad peak centred around 480 cm^{-1}. From the Raman spectra of the films deposited at $w < 35$ W the silicon crystalline phase is clearly identified, while for $w \geq 35$ W the amorphous phase appears to manifest. Raman spectra of the samples deposited by varying the rf power from 10 to 25 W show a well defined peak that downshifts from 520 to 517 cm^{-1} indicating the reduction in the size of the silicon crystallites [17-18]. The spectrum of the film deposited at $w = 35$ W exhibits only a feeble shoulder around 520 cm^{-1}, indicating the presence of smaller silicon crystallites. The evaluation of crystalline volume fraction, f, can be obtained with some caution by the ratio of the integrated scattering intensity of the crystalline phase to the total scattering intensity $f = I_c/(I_c+I_a)$ where I_c and I_a are the areas under the Gaussian peaks at 520 and 480 cm^{-1} respectively [19]. The crystalline fraction as a function of rf power is shown in the inset of the Fig. 1. Fig. 2 represents the XRD spectra of the samples. The spectra of samples deposited with rf power up to 25 W reveal clearly the presence of silicon crystallites while the spectrum of the film deposited at $w = 35$ W has only a small protuberance and the spectra of samples grown at higher rf power exhibit amorphous character. The normalized intensity peak for the diffraction plane (111) of the XRD spectra of samples deposited at $w = 10, 25, 35$ W are

shown in the inset of Fig. 2. The increase in the width of XRD peaks with the increase of rf power indicates the decrease in the crystallite dimension. Neither SiC nor C crystalline phase are observed in the Raman and XRD spectra. The size of the silicon crystallites of the studied films, determined from XRD spectra using Sherrer formula, and the carbon content, x = C/(C+Si), as well as the hydrogen content, obtained from RBS and ERDA respectively, are shown as a function of rf power in Fig. 3. The size of Si crystallites decreases from 15.5 to 7.7 nm with the increases of w from 10 to 35 W. The carbon and the hydrogen contents, on the other hand, increase with the increase in w.

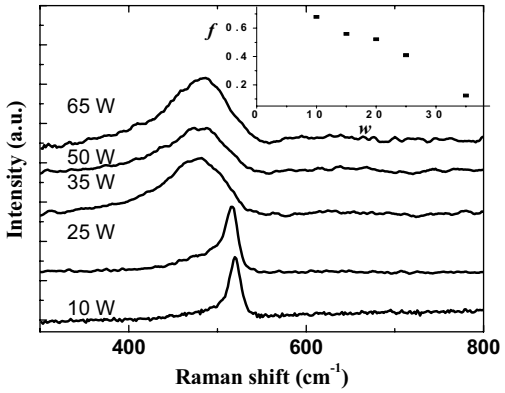

Fig. 1: Raman spectra of the films deposited at different rf power w. In the inset the crystalline fraction f vs. w.

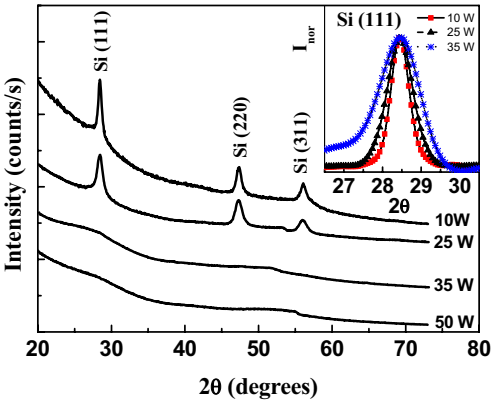

Fig. 2: XRD spectra of the samples deposited at different rf power w. In the inset the normalized intensity peak for the diffraction plane (111) of XRD spectra of the films deposited with w of 10, 25 and 35 W

.

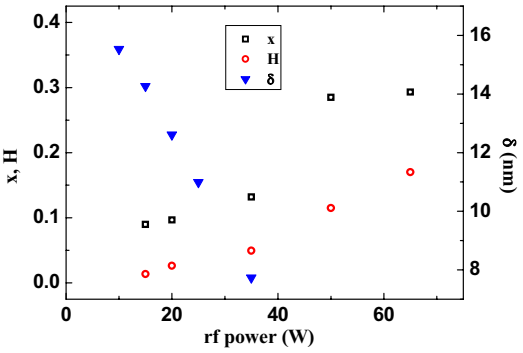

Fig. 3: The size of the silicon crystallites, δ, carbon content, x, and hydrogen content, H, versus the rf power w.

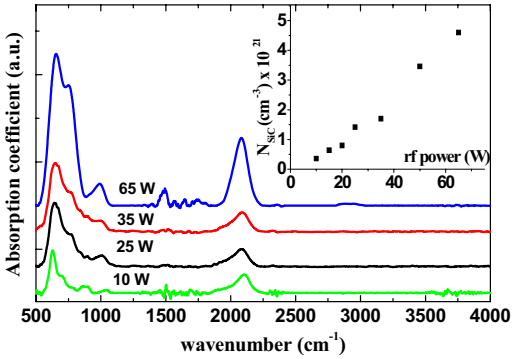

Fig. 4: FTIR spectra of the samples deposited at different rf power w. In the inset the bond density of Si-C stretch, N_{Si-C} vs. w.

FTIR absorption spectra of the samples in the range 400-4000 cm^{-1}, shown in Fig. 4, exhibit the effect of rf power on the bond configurations. The region between 500 and 1000 cm^{-1}, containing the Si-C stretching modes, is essentially the superposition of two main vibration modes centred at 640 cm^{-1} (due to the Si-H wagging/rocking) and around 780 cm^{-1} (ascribed to the Si-C stretching). Other feeble modes in this region are Si-H bending modes in the range 800-900 cm^{-1}. Further the corresponding Si-H stretching mode is observed in the range from 2000 to 2200

cm^{-1}. The Si-C bond density, $N_{Si\text{-}C}$, evaluated from the integrated area of the deconvoluted band near 780 cm^{-1}, using 2.13×10^{19} cm^{-2} as the inverse cross section [20], is shown in the inset of the Fig. 4. From the conspicuous absence of C-H and C-C IR modes, it can be concluded that carbon has been bonded to silicon due to the chemical ordering [21] resulting in the increased number of Si-C stretching modes, with increasing rf power.

Fig. 5 presents the dark conductivity, σ_d, and the photoconductivity, σ_{ph}, at room temperature as a function of rf power. Both quantities exhibit a significant variation with increase in rf power. The dark conductivity decreases rapidly up to w = 35 W and thereafter decreases relatively slowly for w > 35 W. Similar behaviour is observed for the photoconductivity. The changes in the slopes of σ_d and σ_{ph} seem to indicate the existence of two phases. Moreover, it can be seen in the inset of Fig. 5 that the dark conductivity values of the studied films are orders of magnitude higher than those of hydrogenated amorphous silicon carbon films of corresponding carbon content of Ref. [22]. This fact suggests the possible presence of nanocrystallites in the samples deposited for w >35 W even though they appear to be amorphous by Raman and XRD measurements.

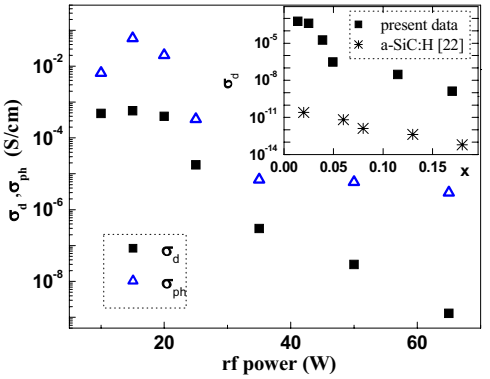

Fig. 5: Room temperature dark conductivity, σ_d, and photoconductivity, σ_{ph}, vs. rf power w. In the inset σ_d, of the studied films and a-SiC:H films of Ref. [22] vs. the carbon content x.

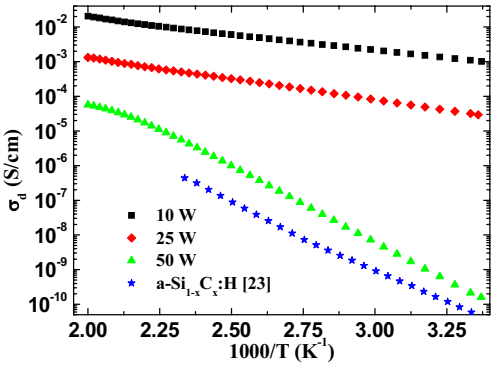

Fig. 6: Dark conductivity, σ_d(T), as a function of 1000/T for the samples deposited at different rf power w and for the hydrogenated amorphous silicon carbon film of Ref. [23] having carbon content of 0.085.

The electrical behaviour of the studied films are found to be correlated with the results of the structural and compositional properties. In fact, higher electrical conductivity (see Fig. 5) is observed for the films, deposited at low rf power, having higher crystalline fraction and lower carbon content. At w = 35 W the crystalline fraction falls to about 0.13 and the amorphous phase seems to dominate for higher rf power. Clearly, the reduction of the silicon crystallite size and crystalline fraction as well as the increase of carbon content appear to influence the electrical behaviour of the films.

To get more information about the transport properties of silicon carbon films, the dark conductivity was measured as a function of the temperature, σ_d(T), in consecutive heating-cooling runs. The conductivity curves measured during the cooling run superimpose with those measured in the heating run after few thermal cycles.

The temperature dependence of the dark conductivity shows a semiconductor like behaviour well fitted by the well known formula

$$\sigma_d(T) = \sigma_o \exp(-E_a/kT)$$

where E_a is the activation energy, σ_o is the conductivity prefactor and k is the Boltzmann constant. Fig.6 exhibits the conductivity $\sigma_d(T)$ versus the inverse temperature for our samples and for the hydrogenated amorphous silicon carbon film reported in the literature [23] having carbon content (x = 0.085) similar to that of the film deposited at 50 W (x = 0.115). σ_d(T) curves of samples deposited by varying rf power tend to shift downward and the slope raises with the increase in w. The analysis reveals that E_a increases from 0.18±0.01 to 0.96±0.01 with increasing rf power from 10 to 65 W. The higher conductivity values for the sample deposited at w = 50 W as compared to those

of hydrogenated amorphous silicon carbon film of similar carbon content for all temperature range corroborate further the presence of nanocrystallites in the studied films. More work is still in progress to better understand this.

4. Conclusion

The structural and electrical properties of the studied films are found to depend strongly on rf power.

The increase of rf power leads to a decrease of silicon crystalline fraction and an increase of the carbon content bonded to silicon in the amorphous matrix. At lower rf power the crystalline fraction and crystallite size appear to be correlated to high electrical conductivity and low activation energy. At higher rf power the amorphous phase seems to be responsible for lower dark conductivity and higher activation energy, furthermore, the presence of silicon nanocrystallites in the films has been revealed from data analysis.

Acknowledgement

We wish to thank dr. M. Passacantando of Università dell'Aquila (Italy) for XRD measurements and many helpful discussions. We (D.K.B. in particular) are thankful and acknowledge the support under ICTP TRIL programme.

References

[1] D. Kruangam in J. Kanicki (ed.), Amorphous and Microcrystalline Semiconductor Devices, Artech House, Boston, 1991, Capter 6
[2] S. Xu, M.B. Yu, Rusli, S. Yoon, C.M. Che, Appl. Phys. Lett 76 (2000) 2550
[3] Y. Matsumoto, G.Hirata, H.Takakura, H. Okamoto, Y. Hamakawa, J. Appl. Phys (1990) 6538
[4] Y. Fujii, A. Hatano, A.Suzuki, M. Yoshida, S. Nakajima, J. Appl Phys. 61 (1987) 1657
[5] R. Martins et al., J. Non Cryst Solids 114 (1989) 486
[6] A. Dasgupta, S.C. Saha, S. Ray, R.Carius, J. Mater. Res. 14 (1999) 2554
[7] F. Damichelis, C.F. Pirrri, E. Tresso, Philos. Mag B, 67 (1993) 331
[8] S. Miyajima, A. Yamada, M. Konegai, Thin Solid Films 430 (2003) 274
[9] U. Coscia, G. Ambrosone, S. Lettieri, P. Maddalena, S. Ferrero Thin Solid Films 511-512 (2006) 399
[10] U. Coscia, et al. Thin Solid Films 515 (2007) 7634-7638.
[11] U. Coscia, G. Ambrosone, D. K. Basa J. Appl. Phys. 103 (2008) 063507
[12] D.K. Basa, G. Ambrosone, U. Coscia, Nanotechnology 19 (2008) 415706
[13] V. Suendo, G. Patriarchi, P. Roca i Cabarrocas, J. Non-cryst. Solids 352 (2006) 1357
[14] S. Zhang, X. Liao, Y. Xu, R. Martins, E. Fortunato, G. Kong, J. Non-cryst. Solids, 338-340 (2004) 188
[15] A. Fontcuberta i Morral, P. Roca i Cabarrocas, Thin Solid Films 383 (2001) 161
[16] G. Conibeer et al., Thin Solid Films 511-512 (2006) 654
[17] Z. Iqbal, a.P. Webb, S. Veprek, Appl. Phys. Lett. 36 (1980) 183
[18] S. Hamma and Roca i Cabarrocas, Solar Energy Mater. & Solar Cells 69 (2001) 217
[19] A. Das Gupta, S. Ghosh, S.T. Khirsagar, S. Ray, Thin Solid Films 295 (1997) 37
[20] D.K. Basa, F.W. Smith, Thin Solid Films 192 (1990) 121
[21] K. Mui, D.K. Basa, F.W. Smith, R. Cordemann, Phys. Rev. B 35 (1987) 8089
[22] U. Coscia, et. al., Thin Solid Films 453-454 (2004) 7
[23] J. Bullot and M.P. Schmidt, Phys Status Sol. b 143 (1987) 343